

1 Early and late evoked brain responses
2 differentially reflect feature encoding and
3 perception in the flash-lag illusion
4

5 Julian Keil^{1,2}, Daniel Senkowski¹, & James K. Moran^{1†}

6 ¹ Department of Psychiatry and Psychotherapy, Multisensory Integration Lab, Charité
7 Universitätsmedizin Berlin, Germany

8 ² Biological Psychology Christian-Albrechts-University Kiel, Kiel, Germany

9 †corresponding author: james-kenneth.moran@charite.de

10

11 **Short title:** Evoked brain correlates of the flash-lag illusion
12

13 **Data availability statement:** Data available upon reasonable request subject to approval from
14 both institutions' ethics committees.
15

16 **Declarations of interest:** The authors declare no competing interests.

17 **Ethics approval statement:** The study was carried out in accordance with the 2008 Declaration
18 of Helsinki and was approved by the ethics commission of the Charité – Universitätsmedizin
19 Berlin (Approval number: EA1/169/11).

20 **Author Contributions:** Study Design: JK, DS, JKM, Data Collection: JKM, Data Analysis:
21 JK; Manuscript preparation: JK, DS, JKM

22 **Acknowledgments:** This research was funded by a grant to DS from the German Research
23 Foundation (SE1859/4- 1). We thank Marianne Bröker, Alex Masurovsky, Teresa Ramme, Lisa
24 Renziehausen, and Joseph Wooldridge for their assistance gathering the data.

25

26

27 **Keywords:** Postdiction, Flash-Lag Illusion, EEG, ERP

28

29 **Highlights:**

30 Flash-lag illusion relates primarily to late evoked brain potentials (>300ms)

31 Illusion vs. no-illusion trials showed difference in fusiform gyrus

32 Flash-lag illusion could involve postdiction-driven integration of ongoing stimuli

33

34 *Abstract:*

35 In the flash-lag illusion (FLI), the position of a flash presented ahead of a moving bar is
36 mislocalized, so the flash appears to lag the bar. Currently it is not clear whether this effect is
37 due to early perceptual-related neural processes such as motion extrapolation or reentrant
38 processing, or due to later feedback processing relating to postdiction, i.e. retroactively altered
39 perception. We presented 17 participants with the FLI paradigm while recording EEG. A central
40 flash occurred either 51ms (“early”) or 16ms (“late”) before the bar moving from left to right
41 reached the screen center. Participants judged whether the flash appeared to the right (“no flash
42 lag illusion”) or to the left (“flash-lag illusion”) of the bar. Using single-trial linear modelling,
43 we examined the influence of timing (“early” vs. “late”) and perception (“illusion” vs. “no
44 illusion”) on flash-evoked brain responses, and estimated the cortical sources underlying the
45 FLI. Perception of the FLI was associated with a late window (368-452ms) in the ERP, with
46 larger deflections for illusion than no illusion trials, localized to the left fusiform gyrus. An
47 earlier frontal and occipital component (200-276ms) differentiated time-locked early vs. late
48 stimulus presentation. Our results suggest a postdiction-related reconstruction of ambiguous
49 sensory stimulation involving late processes in the occipito-temporal cortex, previously
50 associated with temporal integration phenomena. This indicates that perception of the FLI relies
51 on an interplay between ongoing stimulus encoding of the moving bar and feedback processing
52 of the flash, which takes place at later integration stages.

53 **1 Introduction**

54 In our environment, incoming stimuli are continuously integrated into the ongoing stream of
55 sensory inputs, leading to smooth conscious perception. Some perceptual illusions could
56 provide a clue as to how this is performed. In the case of the Flash-Lag illusion (FLI), when a
57 moving object is presented with a briefly flashed stimulus, the moving object is misperceived
58 as being further along its trajectory than it really is (Nijhawan, 1994). Although there are a
59 number of theoretical assumptions regarding the origins of the FLI, many have in common the
60 idea of a designated time window, within which the moving object and the flash could be
61 integrated (Hubbard, 2014). Perception is shaped by input preceding the flash stimulus and
62 there is likely also a time window of a few hundreds of milliseconds within which information
63 that is presented after a stimulus can retroactively affect the perception of this stimulus (Sergent,
64 2018; Shimojo, 2014). Theories differ in terms of the relative weighting of the pre-flash and
65 post-flash sensory processing for the FLI. In a parallel manner, the proposed neural mechanisms
66 underlying these theories are also separate, with some emphasizing early, temporally stimulus-
67 locked processing (e.g. Hogendoorn, 2020) and others emphasizing later stimulus decoupled
68 global processing (Sergent, 2018).

69 Theories focusing on the importance of pre-stimulus sensory processing for perception have
70 linked the FLI to interactions between the higher visual area (V5) and the primary visual cortex
71 (V1). One of the most thoroughly elaborated theories, both in theoretical and empirical terms,
72 is the motion extrapolation theory (Hogendoorn, 2020), in which the window of integration is
73 reflected in higher level visual areas, which are preactivated in anticipation of ongoing
74 movement, as a means of compensating for temporal lags in neural transmission from lower-
75 to higher-level feedforward connections (Hogendoorn & Burkitt, 2019). In these terms there is
76 a disjunct between the anticipated movement of the moving stimulus and the unpredictable
77 onset of the flash stimulus. Recently, Hogendoorn & Burkitt, (2018) contrasted predictable vs.
78 non-predictable moving stimuli and found that the former could be decoded from relatively
79 early EEG activity, i.e., around 140ms after stimulus onset. Moreover, a functional
80 neuroimaging study showed that motion-related stimulus processing in V5 and V1 appears to
81 be subject to predictive coding, with less predictable visual movements producing greater
82 BOLD responses (Schellekens et al., 2016). Another elegant explanation of the FLI is the non-
83 linear latency difference theory (Arstila, 2015), which involves reentrant processing from V5
84 to V1. In this theory, reentrant processing from V5 to V1 is related to conscious perception.
85 The FLI is predicted to stem from a violation of this process: the stimuli create a conflict

86 between the reentrant processing of the early stimulus, i.e., the moving bar, and feedforward
87 processing of the later flash stimulus in V1, leading to the illusory perception of a lagging flash.
88 In sum, there are compelling theories linking FLI to early (<200ms) visual prestimulus
89 processing, tightly coupled to the order of stimulus presentation.

90 In contrast to these theories, the concept of postdiction emphasizes the importance of
91 information that follows the flash. Perception phenomena in which a second stimulus
92 retroactively affects the perception of a first stimulus have been coined postdiction (Shimojo,
93 2014). Foundational findings in support of the postdiction hypothesis come from Eagleman &
94 Sejnowski, (2000), who posit that the window of integration is biased by the subsequent motion
95 of the stimulus. In support of this, the authors demonstrated that the FLI is maintained and can
96 even be further manipulated when only a post-flash movement is present, but far less so when
97 only pre-flash movement is present (Eagleman & Sejnowski, 2007). Postdiction is currently
98 operationally defined, and agnostic as to the underlying neural mechanisms. However,
99 integration across greater timescales, decoupled from the actual temporal order of stimulus
100 presentation, will likely require an involvement of top-down processes (Sergent, 2018). Thus,
101 in contrast to theories of early stimulus-locked neural processing, postdiction is more
102 compatible with global top-down processing at later integration stages.

103 Other temporally governed perceptual phenomena show a split between early and later
104 components in the empirical literature (Förster et al., 2020). They have been invoked to support
105 competing theories. For example, backward-masking shows the dependency of conscious
106 perception on reentrant processing between V5 and V1 (Fahrenfort et al., 2007). However, Cul
107 et al., (2007) found that the difference in backward-masked trials subjectively rated as invisible
108 vs. visible, was not related to early P1 or N1 components, but rather to the later P3 component.
109 In a parallel manner, retroactively altered perception of basic stimuli in the FLI may be
110 dependent on either earlier local-recurrent loops or on later top-down reamplification across
111 wider areas of the brain.

112 A more precise picture of the time course of cortical activation would help clarify the relative
113 strengths of the above theoretical accounts on perception in the FLI. Up until now, however,
114 there has been little investigation of the phenomenon using methods with a fine time resolution,
115 such as EEG or MEG. One EEG study from Stekelenburg & Vroomen, (2005) has shown the
116 effects of an audiovisual manipulation of the visual flash lag, which reduced the flash-lag effect
117 and a correspondingly reduced N1 event-related potential (ERP) component. Moreover, the FLI
118 can be disrupted at approximately 200ms post flash by TMS stimulation of MT+ (Maus et al.,

119 2013). In another EEG study, Chakravarthi & VanRullen (2012) examined the single-trial
120 oscillatory correlates of FLI, showing that the illusion was dependent on the phase of alpha and
121 beta oscillations pre- and post-flash onset, respectively. This suggests the periodic sampling of
122 temporal windows rather than the continuous sampling of individual time points. Still, an ERP
123 study comparing flash-lag vs. non-flash-lag processes directly across a longer time scale is still
124 missing from this literature.

125 In the present study, we examined the ERP components of a FLI, testing directly the difference
126 in the ERPs between stimuli where the flash-lag is perceived and where it is not perceived.
127 Differences in early components (C50, P1, N1 <200ms) would be congruent with theories
128 emphasizing early processing, e.g., motion extrapolation or reentrant processing, whereas
129 differences in later components (>300ms) would support theories that emphasize later feedback
130 processing of postdiction.

131

132 **2 Methods**

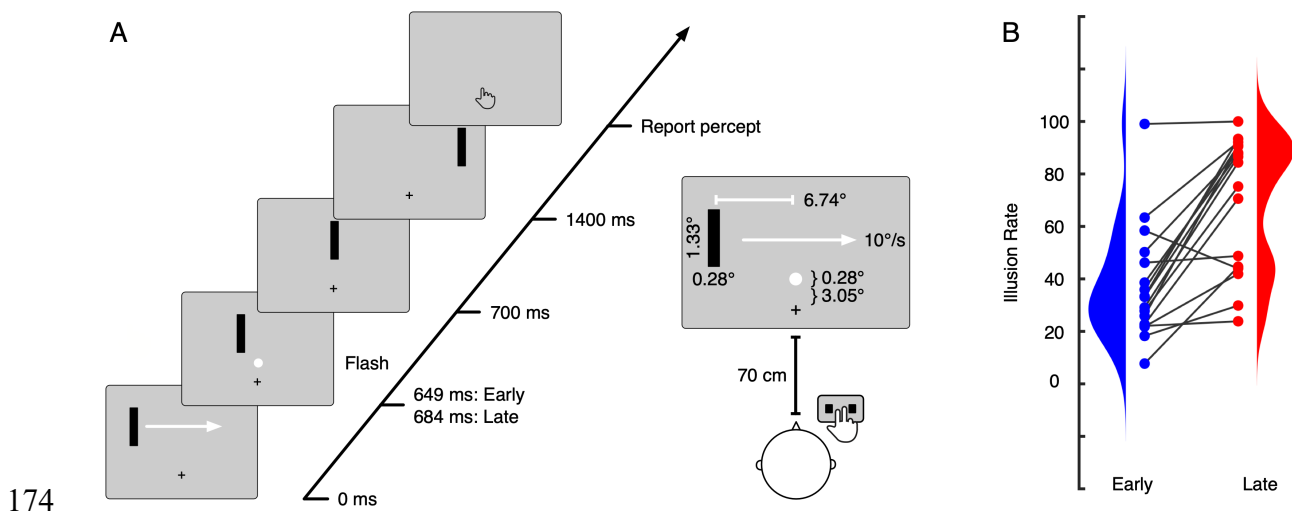
133 *2.1 Participants*

134 An initial sample of 29 paid volunteers participated in this study. All had normal or corrected
135 to normal vision and reported no history of neurological or psychiatric illness. Twelve
136 participants were removed from the sample after participation: Six were excluded due to noisy
137 EEG data or insufficient detection of the catch trials, and six were excluded because they had
138 too few trials in the examined conditions (e.g., too few or too many illusion trials, see below).
139 After preprocessing of the electrophysiological data, 17 participants (8 female, mean age: 38.47
140 (Range: 24-52)) were included in the final data analysis. Handedness 15 were right-handed
141 according to the Edinburgh Handedness Inventory, (Oldfield 1971), with two <50% right-
142 handed. The study was conducted in accordance with the local Ethics Committee of the Charité
143 – Universitätsmedizin Berlin as well as with the 2008 Declaration of Helsinki, and all
144 participants provided written informed consent (Ethical approval number: EA1/169/11).

145 *2.2 Task*

146 Participants were seated in a dimly lit, electrically and acoustically shielded chamber, while
147 being presented with stimuli of the flash-lag paradigm. Participants had to indicate by a button-
148 press whether a visual flash appeared to the right or to the left of a moving bar (Fig. 1A). On a
149 CRT monitor, a black bar ($1.33^\circ \times 0.28^\circ$ visual angle) moved from the left to the right with a
150 speed of 10° visual angle per second for 1400 ms. The distance from the bar onset to the screen
151 center was 6.74° visual angle, and the bar reached the screen center after 700 ms. A fixation
152 cross was presented for the whole trial at the bottom center of the screen. Above the fixation
153 cross (3.05° visual angle), a white circle (0.28° visual angle) flashed for 16.7 ms, either if the
154 bar was 51 ms (*early* trials) or 16 ms (*late* trials) away from reaching the center of the screen.
155 After the bar reached the right side of the screen, the bar remained stationary for 100 ms before
156 disappearing and the fixation cross turned into a hand symbol as a response cue. The response
157 cue ensured that there was no confounding motor activity during the stimulation period. The
158 response interval had a random duration between 1500 ms and 2500 ms. Additional audiovisual
159 trials were presented, which contained a 16.7 ms 72 dB(SPL) white noise burst 100 ms before
160 the bar reached the screen center (Stekelenburg and Vroomen, 2005). These trials were not
161 entered into the data analysis because they were not relevant for the current research question.
162 Overall, the experiment consisted of 200 trials per condition (early flash without a burst; late
163 flash without a burst; early or late flash with noise burst), 168 trials (equally distributed across
164 conditions; ~15% of all presented trials) with a reversed direction (right to left) of the bar

165 movement, and 172 catch trials (equally distributed across conditions; ~15% of all presented
166 trials) in which the central fixation cross was surrounded by a box with the cross within it. This
167 change in catch trials occurred 60 ms before the bar reached the center of the screen and
168 participants were required to respond to the trials by pressing both buttons simultaneously.
169 Trials with a reversed movement were included to avoid habituation effects. Catch trials were
170 included to ensure that participants focused on the central fixation cross. Trials of the different
171 experimental conditions, reversed direction trials, and catch trials were presented in random
172 order. In sum, 1140 trials were presented. Each trial had a duration of 3500 ms, leading to a
173 total experimental runtime of about 66 minutes (divided into 15 blocks).



175 **Figure 1: Experimental setup of visual flash-lag trials and behavioral findings.** (A) A black
176 bar moved from left to right across the screen for 1400 ms. Either 51 or 16 ms before the bar
177 reached the center of the screen, a white circle was flashed for 16.7 ms. Participants had 1500-
178 2500 ms to respond using the right hand. (B) Participants perceived the flash-lag illusion more
179 often when the flash appeared late (i.e., 16.7 ms prior to the bar reaching the center; red)
180 compared to when the flash appeared early (i.e., 51 ms prior to the bar reaching the center;
181 blue).

182 2.3 Behavioral Data Analysis

183 Participants reported their perception with their right hand using a CEDRUS response pad, with
184 a left button pressed by the index finger as the circle appearing 'left' relative to the bar and a
185 right button pressed by the middle finger as the circle appearing 'right' relative to the bar and
186 both buttons simultaneously as soon as the catch trial cue appeared. From the participants'
187 responses, trials were categorized as *illusion trials* if participants reported the central flash on
188 the left of the bar moving from the left to the right of the screen, i.e., if the central flash

189 perceptually lagged the moving bar and as *no illusion trials*, if they correctly reported the flash
190 to be to the right (relative to the moving bar) when the flash was presented.

191 2.4 EEG Data Analysis

192 EEG data were recorded with a high-density 128-channel EEG system (EasyCap, Herrsching,
193 Germany), including one horizontal and one vertical EOG electrode placed below and lateral
194 to the right ocular orbit to register eye movements using Brainamp DC amplifiers
195 (Brainproducts, Gilching, Germany). Recordings were made against nose reference at a
196 sampling frequency of 1000 Hz and with a passband of 0.016–250 Hz.

197 EEG data preprocessing and data analysis were conducted in MATLAB (MathWorks, Natick,
198 MA, USA) using EEGLAB (<http://www.sccn.ucsd.edu/eeglab>) (Delorme & Makeig, 2004),
199 FieldTrip (<http://www.ru.nl/fcdonders/fieldtrip>) (Oostenveld, Fries, Maris, & Schoffelen,
200 2010) and customized scripts. First, data were filtered offline using windowed sinc FIR filters
201 (Widmann et al., 2015) (high pass: 1 Hz, low pass: 125 Hz, notch: 49–51 Hz). Furthermore,
202 data were down sampled to 500 Hz and epochs from – 1 to 1 s relative to flash onset were
203 extracted from the data. Epochs with large artefacts were removed by visual inspection (M
204 removed trials = 222.00, SD = 169.90). To further correct for EOG artefacts (blinks, muscle
205 activity) and strong cardiac activity, independent component analysis (ICA) was conducted
206 (Runica, Lee et al., 1999). On average 3.65 ICA components (SD = 1.32) were removed.
207 Channels with extremely high artifacts were interpolated with distance interpolation (M
208 removed electrodes = 7.65 electrodes, SD = 3.41). The EOG channels were not included in the
209 further analysis of ERPs. For the analysis of ERPs, epochs were lowpass filtered below 45 Hz
210 using windowed sinc FIR filters (Widmann et al., 2015), and the epoch mean was subtracted.
211 For the EEG data analysis only trials in which the bar moved from the left to the right were
212 used. After artifact rejection on average 81.4 (SD +/- 35.27) trials were available (*early illusion*
213 = 119.7 +/- 44.51, *early no illusion* = 47.0 +/- 36.85, *late illusion* = 56.29 +/- 29.83, *late no*
214 *illusion* = 102.64 +/- 37.23).

215 To investigate the cortical sources of the observed ERP responses in the electrode-level
216 analysis, we followed previously established analysis pipelines (Keil et al., 2017; Speer et al.,
217 2020) and performed source localization using a linearly constrained minimum variance
218 (LCMV) beamformer algorithm (VanVeen et al., 1997). A leadfield was generated using a
219 realistic three-shell boundary-element volume conduction model based on the MNI standard
220 brain (MNI; <http://www.mni.mcgill.ca>) for each grid point in the brain on a regular 10-mm grid.
221 Within each participant, we first constructed a common spatial filter across all conditions from

222 the covariance matrix of the averaged single trials at electrode level and the respective leadfield.
223 The use of a common spatial filter for all data guaranteed that differences in source space
224 activity could be ascribed to power differences in the different conditions and not to differences
225 between filters. The lambda regularization parameter was set to 10%, to compensate for
226 potential rank reduction during preprocessing. We then projected the single condition ERPs for
227 the two time-windows identified in the electrode-level analysis into source space using the
228 precomputed common filter. A baseline correction was performed for each time window and
229 condition, using the inverse interval prior to stimulus onset for each time window. To this end,
230 the activity in the respective baseline interval was first subtracted from the post-stimulus
231 interval of interest, and the resulting difference was then divided by the average baseline
232 activity. The anatomical regions of the source localization were determined based on the
233 automated anatomic labelling atlas (AAL, Tzourio-Mazoyer et al., 2002).

234 2.5 Statistical Analyses of EEG Data:

235 The influence of the flash onset latency and the perception of the illusion on the event-related
236 potentials was simultaneously evaluated using single-trial linear models in the first 500 ms after
237 flash onset. In the first level, the single trial amplitude of the ERP was related to the within-
238 subject factors Time (*early vs. late*), Illusion (*illusion vs. no illusion*), and the interaction
239 between both factors in each participant. In the second level, beta values for the two factors and
240 the interaction were compared to zero across participants. To this end, we conducted a non-
241 parametric cluster-based permutation test that addresses the multiple comparison problem by
242 clustering together samples adjacent in time and space (Maris & Oostenveld, 2007). The
243 experimental cluster-based test statistic was evaluated against a permutation distribution in
244 order to test the null hypothesis of no difference between beta values and zero using a two-
245 tailed dependent-samples test. The critical alpha level was set to 0.05. In order to control for
246 multiple comparisons across the 2-dimensional matrix of 126 (electrodes)*251 (samples)
247 comparisons, the clustering algorithm searches for neighboring elements below the critical
248 alpha level and sums the t-values in these clusters. Then the condition labels are shuffled, and
249 the same comparison is computed on the shuffled data. This shuffling step is repeated for 1000
250 iterations, and for each iteration the largest sum of t-values is retained ('maxsum' setting).
251 Finally, the t-value sums in the clusters of the empirical data are compared to the distribution
252 of the clusters obtained in iterations. The p-value for each empirical cluster thus is a percentile
253 indicating the likelihood to obtain a cluster of this size based on randomly shuffled data.
254 Importantly, the clusters obtained in this analysis are not due to any *á priori* selection of a time
255 interval but are the solely based on the empirical data. In order to further compare the ERP

256 between the different factors, trials were averaged within the clusters identified in the previous
257 steps within each participant. Then, we compared ERP amplitudes between *early vs. late* and
258 *illusion vs. no illusion* trials using parametric paired-sample t-tests. Additionally, we correlated
259 the illusion rate with the ERP amplitude using a non-parametric Spearman correlation.
260 Moreover, to explore the possibility of further ERP differences between conditions, we
261 computed a 2x2 repeated-measures ANOVA for the two-dimensional channel by time space
262 with FDR correction for multiple comparisons. The alpha-level was set to 0.05 in all post-hoc
263 exploratory analyses. Bayes Factors were computed (BF10, Rouder et al., 2009) as an indicator
264 of the relative evidence for the H0 and H1 on the power averaged within the clusters identified
265 in the previous steps. A BF10 between 1 and 3 indicates anecdotal support for the alternative
266 hypothesis (H1), whereas a BF10 between 3 and 10, and above 10 indicate respectively
267 moderate and strong support for H1. A BF10 of 1 indicates equal support for H1 and the null
268 hypothesis (H0) while, on the other side, a BF10 between 1/3 and 1, 1/10 and 1/3 and below
269 1/10, provides respectively anecdotal, moderate and strong support for H0 (Aczel et al., 2017).
270 In source space, we again used the aforementioned non-parametric cluster-based permutation
271 test to compare source space activity for the factors Time (*early vs. late*) and Illusion (*illusion*
272 *vs. no illusion*) based on 10000 permutations. Source space activity averaged across identified
273 clusters was again correlated with the illusion rate using a non-parametric Spearman
274 correlation. The alpha-level was again set to 0.05 in all post-hoc exploratory analyses in source
275 space, and Bayes Factors were computed as an indicator of the relative evidence for the H0 and
276 H1.

277 **3 Results**

278 *3.1 Behavior*

279 The likelihood to perceive the FLI was influenced by the temporal distance between the bar and
280 the flash ($t(16) = -5.5091$, $CI = [-0.4551 -0.2022]$, $p < 0.001$, $BF10 = 548.0798$). Replicating
281 the findings previous studies (Stekelenburg & Vroomen, 2005), the occurrence of the early
282 flash (Figure 1B blue, 37.28 ± 21.55 , mean % \pm SD) resulted in less illusions than the late
283 flash (Figure 1B red 70.14 ± 25.30). Participants correctly identified the catch trials (87.04
284 ± 16.88).

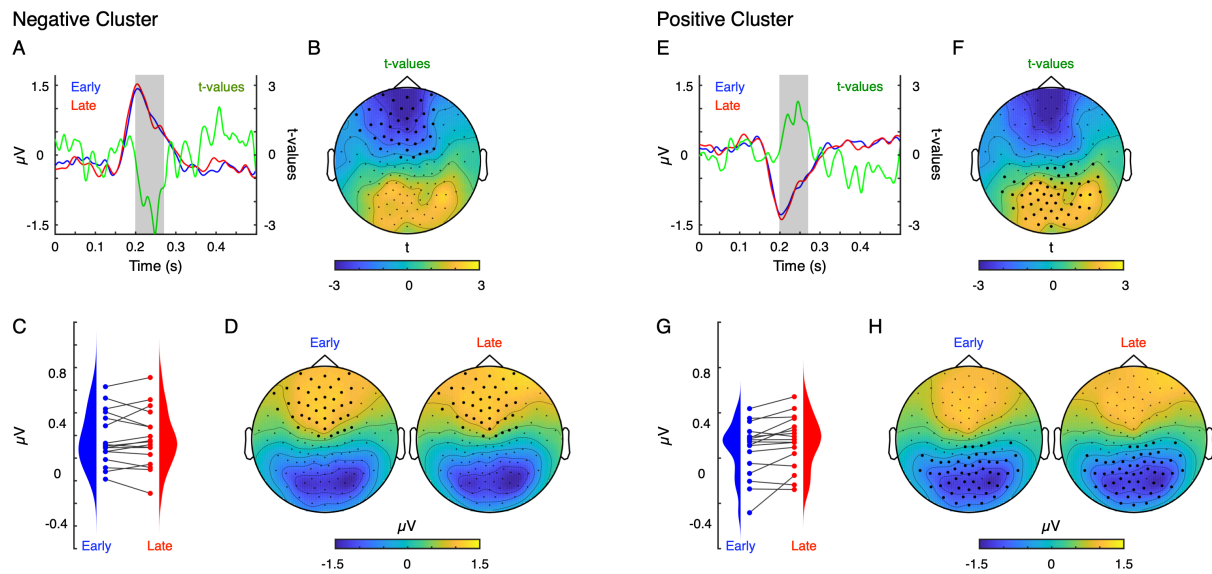
285 *3.2 ERPs*

286 The influence of the flash onset latency and the perception of the illusion on the evoked brain
287 potentials was evaluated using linear modelling within each participant. Then the beta values

288 for the factors Time (*early* vs. *late*), Illusion (*illusion* vs. *no illusion*), and the interaction
289 between the two factors were statistically compared to zero across participants.

290 For the factor Time, the cluster-based permutation test revealed an interval between 200 and
291 276 ms during which the beta values differed from zero. This suggests that in this interval, the
292 single-trial ERPs differ between *early* and *late* trials. Specifically, a cluster of negative beta
293 values was found across frontal electrodes (cluster- $p = 0.005 \pm 0.0044$), and a cluster of
294 positive beta values was found across occipital electrodes (cluster- $p = 0.011 \pm 0.0065$).
295 Averaging the ERP amplitudes across the electrodes of the negative cluster, trials in which the
296 flash occurred early (Figure 2A blue, 0.9257 ± 0.5831 , mean $\mu\text{V} \pm \text{SD}$) compared to trials
297 in which the flash occurred late (Figure 2A red, 0.9310 ± 0.6350) were associated with
298 numerically reduced positive ERP amplitudes. However, this difference was not statistically
299 significant ($t(16) = -0.0991$, $\text{CI} = [-0.1183 \ 0.1077]$, $p = 0.9223$, $\text{BF}_{10} = 0.2500$). Averaged
300 across the positive cluster, trials in which the flash occurred early (Figure 2E blue, $-0.7983 \pm$
301 0.5706) were associated with a numerically less negative ERP amplitudes than trials in which
302 the flash occurred late (Figure 2E red, -0.8149 ± 0.5738). This difference was not significant
303 ($t(16) = 0.3063$, $\text{CI} = [-0.0983 \ 1.1315]$, $p = 0.7633$, $\text{BF}_{10} = 0.2594$). Finally, the correlation
304 analysis between the ERP amplitude averaged over the respective clusters and the illusion rate
305 was not significant (occipital cluster: $r(15) = 0.3971$, $p = 0.1156$, $\text{BF}_{10} = 0.6361$; frontal cluster:
306 $r(15) = -0.3260$, $p = 0.2014$, $\text{BF}_{10} = 0.4146$). Taken together, comparing the beta values
307 obtained from the linear modeling of single-trial ERP amplitudes to zero suggests that ERPs
308 differ between early and late trials. However, the less sensitive comparison between the
309 averages across trials of the two conditions was not significant. Together, this suggests that the
310 difference between early and late conditions is relatively small.

311

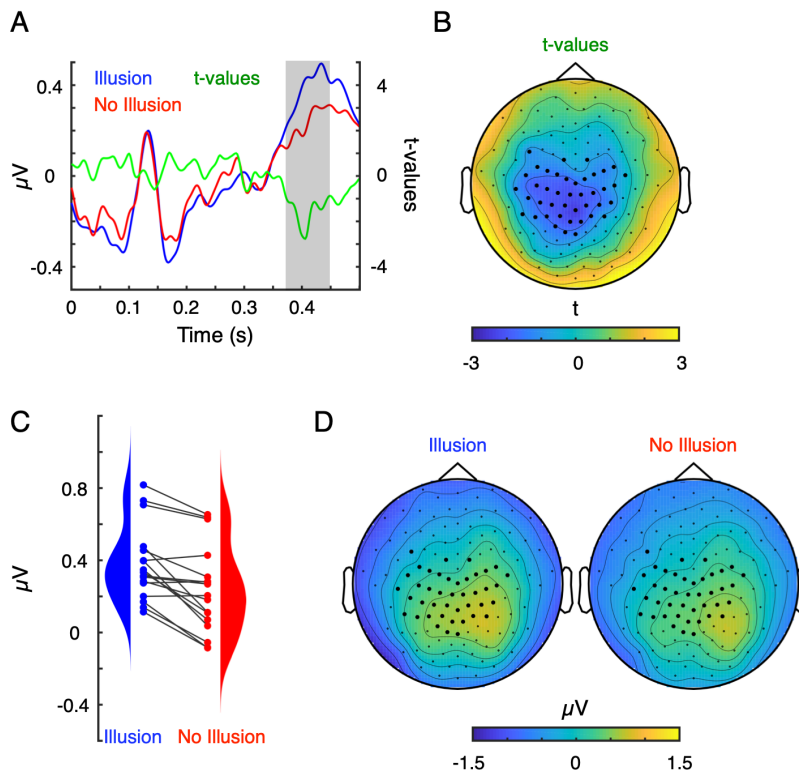


312

313 **Figure 2: Differences between early and late flash-lag trials are reflected in early evoked**
314 **responses.** (A and D) Early (blue) and late (red) flash-lag trials evoked a positive peak around
315 200 ms after flash onset. In the comparison of the beta values from the linear model against
316 zero across participants (green line), an early interval reflected the factor Time. (B) The early
317 interval (200 – 276 ms) comprised a negative cluster across frontal electrodes. (C) Even though
318 the beta values derived from single trials differed significantly from zero, the ERP amplitudes
319 averaged across trials did not differ between early and late trials. (E-H) Same as A-D, but for
320 the positive cluster across occipital electrodes in the same interval.

321 For the factor Illusion, the cluster-based permutation test revealed a late interval between 368
322 and 452 ms during which the beta values differed significantly from zero (Figure 3). This
323 suggests significant single-trial ERPs differences between *illusion* and *no illusion* trials.
324 Specifically, a cluster of negative beta values was found across central electrodes (cluster- $p =$
325 0.02 ± 0.0087). Averaged across the negative cluster, trials in which the participants perceived
326 the FLI were associated with a more positive ERP amplitude (Figure 3A blue, $0.3803 \pm$
327 0.2055) than trials in which participants did not perceive the illusion (Figure 3A red, $0.2339 \pm$
328 0.2410). This difference was statistically significant ($t(16) = 4.8825$, $CI = [0.0828 \ 0.2100]$, $p <$
329 0.001 , $BF_{10} = 181.3138$). Across participants the correlation between the ERP amplitude
330 averaged over the cluster and the illusion rate was not significant ($r(15) = 0.3333$, $p = 0.1910$,
331 $BF_{10} = 0.4311$).

332



333

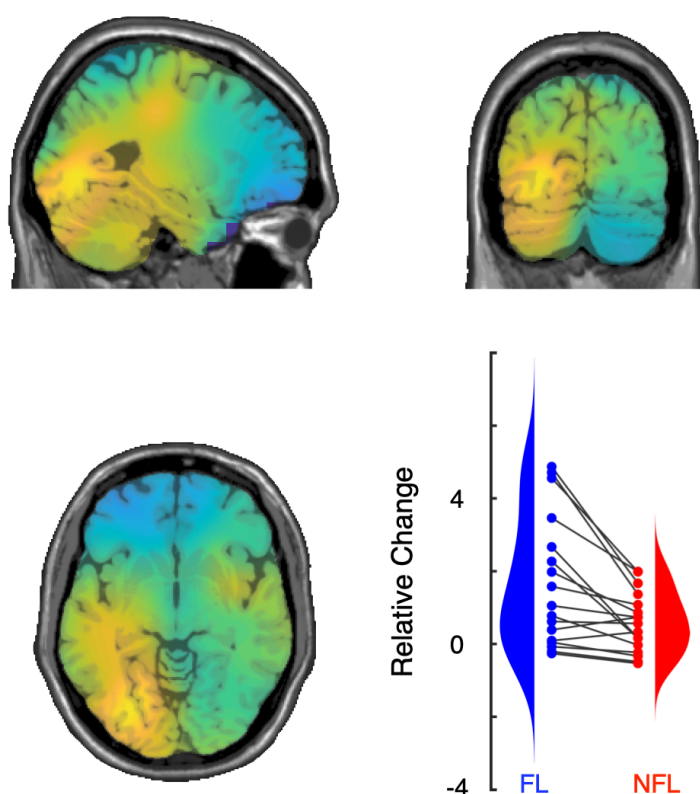
334 **Figure 3: Differences between illusion and no illusion flash-lag trials are reflected in a late**
335 **evoked response.** (A and D) Illusion (blue) and no illusion (red) flash-lag trials evoked a
336 positive peak around 400 ms after flash onset. In the comparison of the beta values from the
337 linear model against zero across participants (green line), a late interval reflected the factor
338 Illusion. (B) The late interval (368 – 452 ms) comprised a negative cluster across central
339 electrodes. (C) The beta values derived from single trials differed significantly from zero, and
340 the ERP amplitudes averaged across trials were more positive for illusion compared to no
341 illusion trials.

342 The exploratory 2x2 repeated-measures ANOVA with the factors Time (early vs. late) and
343 Illusion (*flash-lag* vs. *no flash-lag*) did not reveal any effects. Visual inspection of the
344 uncorrected F and BF10 values indicates short-lived effects, and overall little support for the
345 H1 outside the previously described effects (Supplementary Material).

346 3.3 Source Analyses

347 For the factor Time, the comparison between source space activity for *early* and *late* trials in
348 the 200 to 276 ms interval after stimulus onset did not reveal any significant differences, which
349 is in line with the ERPs analysis (averaged across trials) between conditions at the sensor level.
350 For the factor Illusion the analysis of source space activity revealed an enhanced activity for
351 *illusion* vs. *no illusion* trials in the 368 ms to 452 ms interval (cluster-p = 0.0313 +/- 0.0034;
352 Figure 4). Comparison to the AAL atlas indicated the left inferior occipital gyrus as the primary

353 source of the peak difference. Averaged across the nodes of the cluster, trials in which the
354 participants perceived the FLI (1.6783 +/- 1.8015) were associated with stronger source space
355 signal change from baseline than trials in which participants did not perceive the illusion
356 (0.5888 +/- 0.8211). This difference was statistically significant ($t(16) = 3.6991$, $CI = [0.4651$
357 $1.7139]$, $p = 0.0019$, $BF_{10} = 21.3389$). Across participants there was no significant correlation
358 between the ERP amplitudes averaged over the cluster and the illusion rates ($r(15) = 0.1961$, p
359 $= 0.4492$, $BF_{10} = 0.2442$).



360
361 **Figure 4: Source analysis for the factor Illusion revealed an involvement of the left**
362 **fusiform gyrus.** The comparison of source-space activity indicated an occipital cluster where
363 trials in which participants perceived the flash-lag illusion evoked a stronger signal change from
364 baseline than trials in which they did not perceive the illusion.

365 4 Discussion

366 In our study, we used ERPs to clarify the temporal and spatial neural correlates of the FLI.
367 Some theories predict earlier, stimulus-dependent temporal processing, and others later
368 stimulus-independent temporal processing. We conducted this analysis on a large pool of
369 participants, from which we selected those with an approximately bistable perception of the
370 illusion. A late positive ERP component (368-452ms after the flash onset), localized to the

371 inferior occipito-temporal cortex differentiated between illusion and no illusion perception
372 trials. Illusion trials evoked larger evoked cortical responses than trials in which no illusion
373 occurred. Moreover, in our study, FLI perception was higher in late vs. early trials, with
374 corresponding differences in an earlier ERP component (200-276ms).

375 We found evidence for the influence of late modulation in FLI, which indicates that late
376 processing in the inferior occipital cortex is an important neural origin where perception in the
377 FLI is reconstructed. Thus, later ERP components (>300ms, e.g. P300), which are typically
378 associated with higher-order cognitive (Huang et al., 2015) or post-perceptual processes
379 (Schröder et al., 2021) seem to be critical for the difference between illusion and no illusion
380 perception, at least in our paradigm. This is consistent with a more global processing of visual
381 information in the FLI, temporally decoupled from the stimulus sequence (Shimojo, 2014;
382 Sergent, 2018). One possible interpretation of these results is that attention can modulate the
383 strength of the FLI. For example, the FLI is increased when attentional resources are reduced,
384 such as in a dual-task condition (Sarich et al., 2007) or spatial attention (Baldo et al., 2002).
385 However, top-down attention typically produces enlarged ERPs components in primary sensory
386 regions (Keil et al., 2017; Lange et al., 2008), which is difficult to reconcile with our results, in
387 which larger ERP components are associated with FL rather than NFL. In summary, our
388 findings show that late ERP components differentiate between illusion and no illusion
389 perceptions, which supports the postdiction view on the FLI.

390 Our results are less congruent with theories that postulate early visual processing as critical to
391 the FLI, such as the motion extrapolation (Hogendoorn, 2020) and reentrant based non-linear
392 motion integration (Arstila, 2015). Visual inspection suggests small differences in early
393 components, and Bayes Factors argues against the interpretation of a meaningful difference in
394 early components < 200ms. However, it is also possible that there are important early effects
395 that are too subtle to detect with our sample size. On the face of it, this is difficult to reconcile
396 with the empirical findings that the FLI can be disrupted at approximately 200ms post flash by
397 TMS stimulation of MT+ (Maus et al., 2013). However, this may mean that early activity is
398 necessary for later processing of the visual stimuli, but not sufficient for the perception of the
399 illusion, or that early activity is correlated with later processing rather than being causally
400 necessary (Sergent, 2018). In support of this, we observe that there were differences between
401 the early and late onset flashes at 200 ms to 276ms, which suggests that processing at this time
402 relates to the registration of differences between the physical properties of the stimuli, rather
403 than the FLI itself. Thus, interference with this physical coregistration of stimuli could disrupt
404 upstream perception of the FLI. In all, our results do not appear to reflect the early stimulus-

405 locked processing predicted by motion extrapolation or non-linear motion integration. The FLI
406 dependent on later neural processing steps, decoupled from the temporal order of stimulus
407 presentation.

408 Information regarding the cortical areas involved in the reconstruction of visual perception in
409 the FLI come from our source analysis. This analysis highlighted important regions in FLI
410 processing in approximately left fusiform gyrus. Activity in this region, including later ERP
411 activity has been associated with a heterogenous group of spatial and temporal integrative
412 phenomena. Previously, Meyer & Olson, (2011) found that inferotemporal cells in monkeys
413 were sensitive to violations of statistical regularities in sequentially presented stimuli. Sequence
414 representation has been generalized to encompass various linguistic phenomena (Dehaene et
415 al., 2015). In a broader view, inferior temporal areas have been implicated as a part of a
416 subcortical-extrastriate-fronto-parietal network necessary for the conscious perception of
417 bistable stimuli (Bisenius et al., 2015). Integrating FLI with these models of sensory integration
418 in this region could provide a new way of understanding the FLI phenomenon.

419 The study has some limitations. Our sample was restricted to those remaining participants with
420 a more balanced number of illusion and no illusion trials, so it is possible that the current
421 findings are not generalizable to the other participants. Future studies could adapt the flash
422 onset to individual perception thresholds to ensure a larger sample size (as in e.g. Chakravarthi
423 & VanRullen, 2012). Connected with this, the ERPs were based on a relatively small number
424 of trials per person. It may also be that these factors contributed to the absence of earlier effects
425 in the present study. Nevertheless, the sensitivity of the single-trial linear modelling combined
426 with robust clustering statistics provide reason for confidence in the significant later ERP
427 components. Our source analysis with EEG and non-individualized MRI templates is limited
428 in spatial resolution, and future studies involving e.g. fMRI or MEG, would be necessary to
429 strengthen these findings. Our primary stimuli went left to right, which is congruent with
430 reading stimuli, this may in part explain the activation in the fusiform gyrus. Future studies
431 could build on these findings by ERPs with different types of flash lag variants to test the
432 generalizability of these findings. Furthermore, an attention manipulation could help
433 unconfound potential effects (Koch & Tsuchiya, 2012; Koivisto, Kainulainen, & Revonsuo,
434 2009; Moran et al., in press). Overall, we believe that these limitations do not substantially
435 affected our main finding that late evoked potentials reflect perception-related processing in the
436 FLI. Nevertheless, they should be considered in further research studies examining the neural
437 signatures of the FLI.

438 4.1 Conclusion

439 Our study shows for the first time the time-course of neural activity of the FLI, differentiating
440 illusion from non-illusion trials. Although the different theories posited to explain FLI likely
441 all have some purchase on the truth of this complex phenomenon, our results argue for a greater
442 focus on later postdictive processing, decoupled from the order of stimulus presentation.

443

444 5 References

445 Aczel, B., Palfi, B., & Szaszi, B. (2017). Estimating the evidential value of significant results
446 in psychological science. *PLoS One*, *12*(8), e0182651.

447 Arstila, V. (2015). Keeping postdiction simple. *Consciousness and Cognition*, *38*, 205–216.
448 <https://doi.org/10.1016/j.concog.2015.10.001>

449 Baldo, M. V. C., Kihara, A. H., Namba, J., & Klein, S. A. (2002). Evidence for an Attentional
450 Component of the Perceptual Misalignment between Moving and Flashing Stimuli. *Perception*,
451 *31*(1), 17–30. <https://doi.org/10.1068/p3302>

452 Bisenius, S., Trapp, S., Neumann, J., & Schroeter, M. L. (2015). Identifying neural correlates
453 of visual consciousness with ALE meta-analyses. *NeuroImage*, *122*(C), 177–187.
454 <http://doi.org/10.1016/j.neuroimage.2015.07.070>

455 Chakravarthi, R., & VanRullen, R. (2012). Conscious updating is a rhythmic process.
456 *Proceedings of the National Academy of Sciences*, *109*(26), 10599–10604.
457 <https://doi.org/10.1073/pnas.1121622109>

458 Cul, A. D., Baillet, S., & Dehaene, S. (2007). Brain Dynamics Underlying the Nonlinear
459 Threshold for Access to Consciousness. *PLOS Biology*, *5*(10), e260.
460 <https://doi.org/10.1371/journal.pbio.0050260>

461 Dehaene, S., Meyniel, F., Wacongne, C., Wang, L., & Pallier, C. (2015). The Neural
462 Representation of Sequences: From Transition Probabilities to Algebraic Patterns and
463 Linguistic Trees. *Neuron*, *88*(1), 2–19. <https://doi.org/10.1016/j.neuron.2015.09.019>

464 Delorme, A., & Makeig, S. (2004). EEGLAB: an open source toolbox for analysis of single-
465 trial EEG dynamics including independent component analysis. *Journal of Neuroscience*
466 *Methods*, *134*(1), 9-21.

467 Eagleman, D. M., & Sejnowski, T. J. (2000). Motion integration and postdiction in visual

- 468 awareness. *Science*, 287(5460), 2036–2038. <https://doi.org/10.1126/science.287.5460.2036>
- 469 Eagleman, D. M., & Sejnowski, T. J. (2007). Motion signals bias localization judgments: A
470 unified explanation for the flash-lag, flash-drag, flash-jump, and Frohlich illusions. *Journal of*
471 *Vision*, 7(4), 1–12. <https://doi.org/10.1167/7.4.3>
- 472 Fahrenfort, J. J., Scholte, H. S., & Lamme, V. A. F. (2007). Masking Disrupts Reentrant
473 Processing in Human Visual Cortex. *Journal of Cognitive Neuroscience*, 19(9), 1488–1497.
474 <https://doi.org/10.1162/jocn.2007.19.9.1488>
- 475 Förster, J., Koivisto, M., & Revonsuo, A. (2020). ERP and MEG correlates of visual
476 consciousness: The second decade. *Consciousness and Cognition*, 80, 102917.
477 <https://doi.org/10.1016/j.concog.2020.102917>
- 478 Hogendoorn, H. (2020). Motion Extrapolation in Visual Processing: Lessons from 25 Years of
479 Flash-Lag Debate. *Journal of Neuroscience*, 40(30), 5698–5705.
480 <https://doi.org/10.1523/JNEUROSCI.0275-20.2020>
- 481 Hogendoorn, H., & Burkitt, A. N. (2018). Predictive coding of visual object position ahead of
482 moving objects revealed by time-resolved EEG decoding. *NeuroImage*, 171, 55–61.
483 <https://doi.org/10.1016/j.neuroimage.2017.12.063>
- 484 Hogendoorn, H., & Burkitt, A. N. (2019). Predictive Coding with Neural Transmission Delays:
485 A Real-Time Temporal Alignment Hypothesis. *ENeuro*, 6(2).
486 <https://doi.org/10.1523/ENEURO.0412-18.2019>
- 487 Huang, W.-J., Chen, W.-W., & Zhang, X. (2015). The neurophysiology of P 300--an integrated
488 review. *European Review for Medical and Pharmacological Sciences*, 19(8), 1480–1488.
- 489 Hubbard, T. L. (2014). The flash-lag effect and related mislocalizations: Findings, properties,
490 and theories. *Psychological Bulletin*, 140(1), 308–338. <https://doi.org/10.1037/a0032899>
- 491 Keil, J., Pomper, U., Feuerbach, N., & Senkowski, D. (2017). Temporal orienting precedes
492 intersensory attention and has opposing effects on early evoked brain activity. *NeuroImage*,
493 148, 230–239. <https://doi.org/10.1016/j.neuroimage.2017.01.039>
- 494 Koch, C., & Tsuchiya, N. (2012). Attention and consciousness: Related yet different. *Trends in*
495 *Cognitive Sciences*, 16(2), 103–105. <https://doi.org/10.1016/j.tics.2011.11.012>
- 496 Koivisto, M., Kainulainen, P., & Revonsuo, A. (2009). The relationship between awareness and
497 attention: Evidence from ERP responses. *Neuropsychologia*, 47(13), 2891–2899.
498 <https://doi.org/10.1016/j.neuropsychologia.2009.06.016>

- 499 Lange, D., P, F., Jensen, O., Bauer, M., & Toni, I. (2008). Interactions between posterior
500 gamma and frontal alpha/beta oscillations during imagined actions. *Frontiers in Human*
501 *Neuroscience*, 2. <https://doi.org/10.3389/neuro.09.007.2008>
- 502 Lee, T. W., Girolami, M., & Sejnowski, T. J. (1999). Independent component analysis using an
503 extended infomax algorithm for mixed subgaussian and supergaussian sources. *Neural*
504 *Computation*, 11(2), 417–441.
- 505 Maris, E., & Oostenveld, R. (2007). Nonparametric statistical testing of EEG-and MEG-data.
506 *Journal of Neuroscience Methods*, 164(1), 177-190.
- 507 Maus, G. W., Fischer, J., & Whitney, D. (2013). Motion-Dependent Representation of Space
508 in Area MT+. *Neuron*, 78(3), 554–562. <https://doi.org/10.1016/j.neuron.2013.03.010>
- 509 Meyer, T., & Olson, C. R. (2011). Statistical learning of visual transitions in monkey
510 inferotemporal cortex. *Proceedings of the National Academy of Sciences*, 108(48), 19401–
511 19406. <https://doi.org/10.1073/pnas.1112895108>
- 512 Moran, J.K., Keil, J., Masurovsky, A., Gutwinski, S., Montag, C., & Senkowski, D. (in press).
513 Multisensory processing can compensate for top-down attention deficits in schizophrenia.
514 *Cerebral Cortex*.
- 515 Nijhawan, R. (1994). Motion extrapolation in catching. *Nature*, 370(6487), 256–257.
516 <https://doi.org/10.1038/370256b0>
- 517 Oldfield, R. C. (1971). The assessment and analysis of handedness: the Edinburgh inventory.
518 *Neuropsychologia*, 9(1), 97-113.
- 519 Oostenveld, R., Fries, P., Maris, E., & Schoffelen, J. M. (2010). FieldTrip: Open source
520 software for advanced analysis of MEG, EEG, and invasive electrophysiological data.
521 *Computational Intelligence and Neuroscience*, 2011, 156869-156869.
- 522 Rouder, J. N., Speckman, P. L., Sun, D., Morey, R. D., & Iverson, G. (2009). Bayesian t tests
523 for accepting and rejecting the null hypothesis. *Psychonomic Bulletin & Review*, 16(2), 225-
524 237.
- 525 Sarich, D., Chappell, M., & Burgess, C. (2007). Dividing attention in the flash-lag illusion.
526 *Vision Research*, 47(4), 544–547. <https://doi.org/10.1016/j.visres.2006.09.029>
- 527 Schellekens, W., van Wezel, R. J. A., Petridou, N., Ramsey, N. F., & Raemaekers, M. (2016).
528 Predictive coding for motion stimuli in human early visual cortex. *Brain Structure and*
529 *Function*, 221(2), 879–890. <https://doi.org/10.1007/s00429-014-0942-2>

530 Schröder, P., Nierhaus, T., & Blankenburg, F. (2021). Dissociating perceptual awareness and
531 postperceptual processing: The P300 is not a reliable marker of somatosensory target detection.
532 *The Journal of Neuroscience*. <http://doi.org/10.1523/JNEUROSCI.2950-20.2021>

533 Sergent, C. (2018). The offline stream of conscious representations. *Philosophical Transactions*
534 *of the Royal Society B: Biological Sciences*, 373(1755), 20170349.
535 <https://doi.org/10.1098/rstb.2017.0349>

536 Shimojo, S. (2014). Postdiction: Its implications on visual awareness, hindsight, and sense of
537 agency. *Frontiers in Psychology*, 5. <https://doi.org/10.3389/fpsyg.2014.00196>

538 Stekelenburg, J. J., & Vroomen, J. (2005). An event-related potential investigation of the time-
539 course of temporal ventriloquism. *NeuroReport*, 16(6), 641–644.

540 Tzourio-Mazoyer, N., Landeau, B., Papathanassiou, D., Crivello, F., Etard, O., Delcroix, N., ...
541 & Joliot, M. (2002). Automated anatomical labeling of activations in SPM using a macroscopic
542 anatomical parcellation of the MNI MRI single-subject brain. *Neuroimage*, 15(1), 273-289.

543 Widmann, A., Schröger, E., & Maess, B. (2015). Digital filter design for electrophysiological
544 data--a practical approach. *Journal of Neuroscience Methods*, 250, 34–46.
545 <http://doi.org/10.1016/j.jneumeth.2014.08.002>

546 Van Veen, B. D., van Drongelen, W., Yuchtman, M., & Suzuki, A. (1997). Localization of
547 brain electrical activity via linearly constrained minimum variance spatial filtering. *IEEE*
548 *Transactions on Bio-Medical Engineering*, 44(9), 867–880. <http://doi.org/10.1109/10.623056>

549

550

551

552

553

554

555

556

557

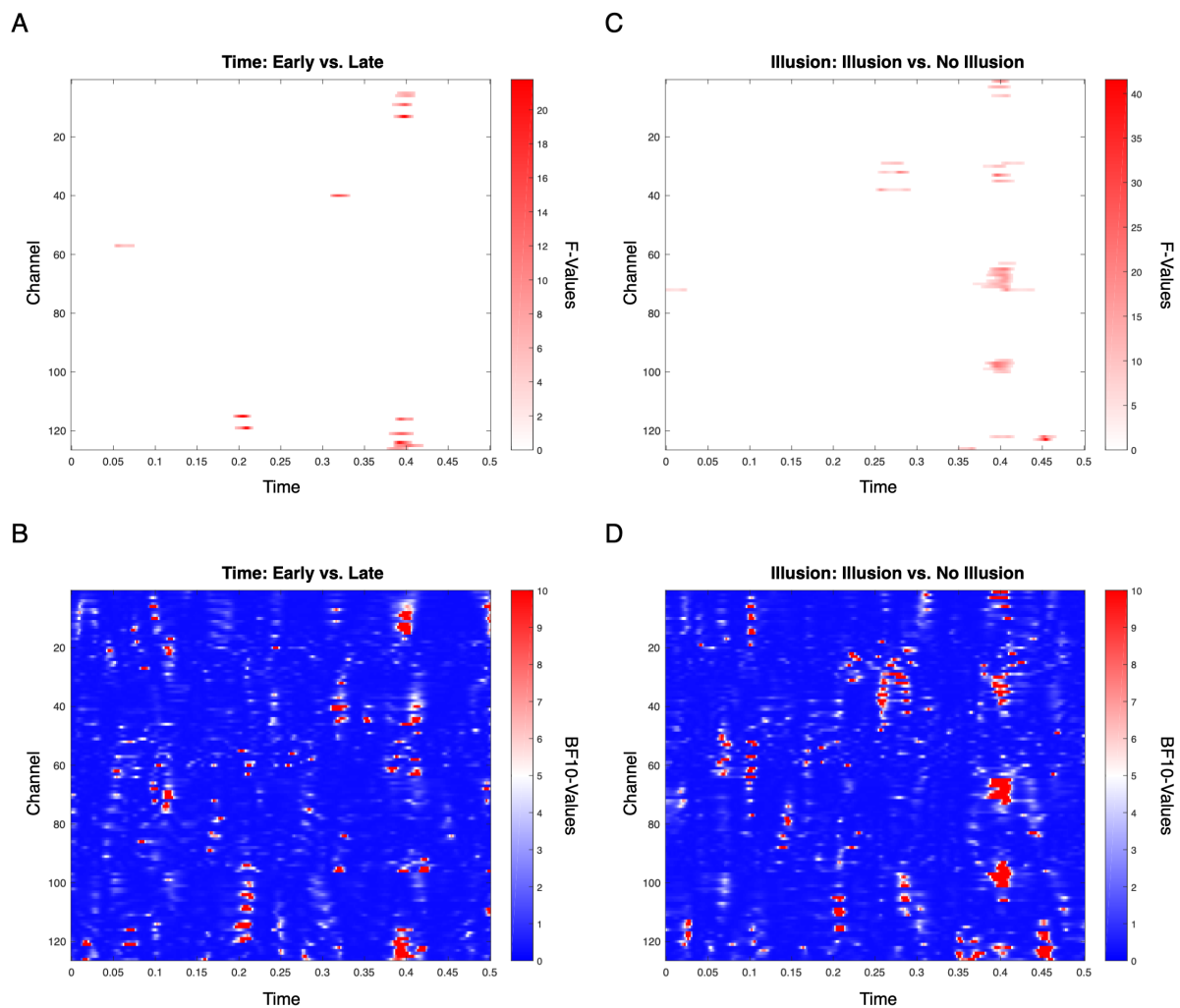
558

559 6 Supplementary Material

560

561 The exploratory 2x2 repeated-measures ANOVA with the factors Time (*early vs. late*) and
562 Illusion (*flash-lag vs. no flash-lag*) did not reveal any effects following FDR correction for
563 multiple comparisons. Visual inspection of the uncorrected F and BF10 values indicates short-
564 lived effects, and overall little support for the H1 outside the previously described effects.

565



566

567 **Supplementary Figure:** The exploratory 2x2 ANOVA did not reveal any effects outside the
568 two intervals reported in the linear model analysis. (A) For the factor Time, F-values masked
569 by the uncorrected threshold of $p < 0.05$ only reveal scattered peaks. (B) Similarly, BF10-
570 values are low, indicating little support for the H1. (C and D) Same as A and B but for the
571 factor Illusion.

572